

Fig. 3. MLE of scattering potential based image using imaging function (16) and the measurement at 5 GHz.

by (16). To make the two images comparable, we normalized the functions of the two images to $[0, 1]$. It can be seen that the scatterer located at $(202.7, 32.3)$ appears in Fig. 2 to be much darker compared with the scatterer at $(224.7, -14.0)$, whereas it is much brighter in Fig. 3. This difference verifies the near-far problem of the basic time-reversal and confirms that the MLE of scattering potential imaging is more balanced due to the proper scaling. In addition, many spurious local peaks can be observed in both images, which are the grating lobes since both the transmit and receive arrays in the experiment have antenna spacing much larger than half of the wavelength. We proposed a wideband imaging approach to exploit frequency diversity and resolved this spatial ambiguity under the sparse array setup. Interested readers are referred to [1].

VI. CONCLUSION

We demonstrated that basic time-reversal imaging is related to an MLE of the scattering potential under the assumption of a simplified single-scatterer physical model. We showed that the two imaging functions differ by a scaling factor, which is function of the imaging position. The basic time-reversal imaging exhibits the near-far problem, producing a weaker image for the area further away from the imaging array, whereas the MLE-based imaging is balanced due to the proper scaling.

ACKNOWLEDGMENT

The authors would like to thank J. M. F. Moura, D. Stancil, and J. Zhu for providing them with the experimental data in Section V.

REFERENCES

[1] G. Shi and A. Nehorai, "Maximum likelihood estimation of point scatterers for computational time-reversal imaging," *Commun. Inf. Syst.*, vol. 5, no. 2, pp. 227–256, 2005.
 [2] M. Fink, "Time-reversed acoustics," *Sci. Amer.*, vol. 281, pp. 91–97, Nov. 1999.
 [3] M. Fink, D. Cassereau, A. Derode, C. Prada, P. Roux, M. Tanter, J. L. Thomas, and F. Wu, "Time-reversed acoustics," *Rep. Progr. Phys.*, vol. 63, pp. 1933–1995, 2000.
 [4] M. Fink and C. Prada, "Acoustic time-reversal mirrors, topical review," *Inverse Problems*, vol. 17, pp. R1–R38, 2001.
 [5] L. Borcea, G. Papanicolaou, and C. Tsogka, "Theory and applications of time reversal and interferometric imaging," *Inverse Problems*, vol. 19, pp. 5139–5164, 2003.

[6] L. Borcea, C. Tsogka, G. Papanicolaou, and J. Berryman, "Imaging and time reversal in random media," *Inverse Problems*, vol. 18, pp. 1247–1279, 2002.
 [7] J. H. Taylor, *Scattering Theory*. New York: Wiley, 1972.
 [8] R. G. Newton, *Scattering Theory of Waves and Particles*. New York: McGraw-Hill, 1966.
 [9] J. W. Brewer, "Kronecker products and matrix calculus in system theory," *IEEE Trans. Circuits Syst.*, vol. cas-52, no. 9, pp. 772–781, Sep. 1978.
 [10] G. B. Arfken and H. J. Weber, *Mathematical Methods for Physicists*, 6th ed. Burlington, MA: Elsevier Academic, 2005.
 [11] A. J. Devaney, Super-Resolution Processing of Multi-Static Data Using Time Reversal and MUSIC, 2000 [Online]. Available: <http://www.ece.neu.edu/faculty/devaney>
 [12] C. Prada and J. Thomas, "Experimental subwavelength localization of scatterers by decomposition of the time reversal operator interpreted as a covariance matrix," *J. Acoust. Soc. Amer.*, vol. 114, pp. 235–243, 2003.
 [13] P. Stoica and A. Nehorai, "MUSIC, maximum likelihood and Cramér-Rao bound," *IEEE Trans. Acoust., Speech, Signal Process.*, vol. ASSP-37, pp. 720–741, May 1989.
 [14] A. J. Devaney, "Basic time reversal imaging of CMU data set," 2004, DARPA progress rep.

$$\begin{matrix} \mathbf{S} & \mathbf{D} & \mathbf{E} & \mathbf{U} \\ \mathbf{S} & \mathbf{P} & & \end{matrix}$$

Fang Yao and Thomas C. M. Lee, Senior Member, IEEE

Abstract—Time reversal imaging is a technique that uses the time reversal property of waves to focus energy on a scatterer. This paper studies the near-far problem of time reversal imaging and proposes a wideband imaging approach to resolve this problem. The proposed approach exploits frequency diversity and resolves the spatial ambiguity under the sparse array setup. The proposed approach is compared with the basic time reversal imaging and the MLE-based imaging. The results show that the proposed approach is more balanced than the basic time reversal imaging and the MLE-based imaging.

Index Terms—Basic time reversal imaging, MLE-based imaging, near-far problem, wideband imaging approach.

I. INTRODUCTION

In this correspondence, we study the problem of nonparametric spectral density estimation. In particular we propose using the so-called *data sharpening* technique [2], [3], [6] to help reduce the estimation bias. Data sharpening can be seen as a data preprocessing step that aims to achieve the following. It produces preprocessed data in such a way that when these preprocessed data are fed into certain standard and relatively simple estimation methods, the results are improved relative to the case when the original raw data were used. In other words, data sharpening can be applied to boost the performances of simple estimation methods while at the same time preserve the simplicity of such methods.

Manuscript received May 10, 2006; revised December 20, 2006. The associate editor coordinating the review of this manuscript and approving it for publication was Dr. Peter Handel.

F. Yao is with the Department of Statistics, University of Toronto, Toronto, ON M5S 3G3, Canada (e-mail: fyao@utstat.toronto.edu).

T. C. M. Lee is with the Department of Statistics, the Chinese University of Hong Kong, Shatin, N.T., Hong Kong and Department of Statistics, Colorado State University, Fort Collins, CO 80523-1877 USA (e-mail: tlee@sta.cuhk.edu.hk).

Digital Object Identifier 10.1109/TSP.2007.896297

Data sharpening procedures have been constructed and studied in the contexts of probability density estimation [2], [6] and nonparametric regression [3]. Here, we extend and improve this technique in the following three directions. First, we apply data sharpening to a different estimation problem, namely, spectral density estimation, by proposing a sharpening procedure for preprocessing the periodogram of a stationary series. Second, unlike those “fixed” sharpening procedures previously studied in [2], [3], and [6], we introduce a tuning parameter in this new periodogram sharpening procedure that allows the data to be “sharpened” to different degrees. “Sharpened periodograms” produced from this procedure can be smoothed, say, by kernel methods to obtain nonparametric estimates of the spectrum of the series. Lastly, based on the idea of unbiased risk estimation, we develop an automatic method for simultaneously choosing the amounts of smoothing and sharpening. To the best of our knowledge, no automatic method has been proposed in the literature for selecting the amount of smoothing for any type of sharpened data. Furthermore, under some mild regularity conditions, we show that the estimate obtained from smoothing the sharpened periodogram enjoys a higher order bias reduction relative to the estimate obtained from smoothing the raw periodogram.

The rest of this correspondence is organized as follows. Background material is reviewed in Section II. Section III defines sharpened periodograms and illustrates its uses for spectral density estimation. Section IV discusses implementation issues. Theoretical and numerical results of our work are presented in Sections V and VI, respectively. Concluding remarks are offered in Section VII. Lastly proofs and technical details are deferred to the Appendix.

II. BACKGROUND

Suppose x_0, \dots, x_{2n-1} is a finite-sized realization of a real-valued, zero-mean stationary process $\{x_t\}$ with unknown spectral density f . Given the observations x_t ,

(h, α) as the pair that minimizes the resulting estimator. We have developed such an estimator, as follows:

$$\hat{R}(h, \alpha) = \frac{\text{RSS}(h, \alpha)}{n} + \frac{1}{n} \sum_{j=0}^{n-1} \left[2 \left\{ (1 + \alpha)W_0 - \alpha \sum_{m=-n}^{2n-1} W_{m-j}^2 \right\} - 1 \right] \frac{I_j^2}{2} \quad (7)$$

where $\text{RSS}(h, \alpha) = \sum_{j=0}^n (I_j - \tilde{f}_{j,\alpha})^2$ is the residual sum of squares. The first term can be treated as a measure for the bias of $\tilde{f}_{j,\alpha}$, while the second term is for the variance. It is shown in Theorem 2 (see Section V) that $\hat{R}(h, \alpha)$ is an unbiased estimator for $R(h, \alpha)$. We propose choosing (h, α) as the joint minimizer of $\hat{R}(h, \alpha)$.

The above idea of data sharpening has been applied to the context of nonparametric function estimation by [3]. However, in [3], the authors only considered the case when $\alpha = 1$ and did not provide any automatic method for choosing h . Thus, in addition to extending the data sharpening technique to periodogram smoothing, we have also advanced the sharpening technique by i) allowing the extent of sharpening to be varied via the introduction of the sharpening parameter α in the

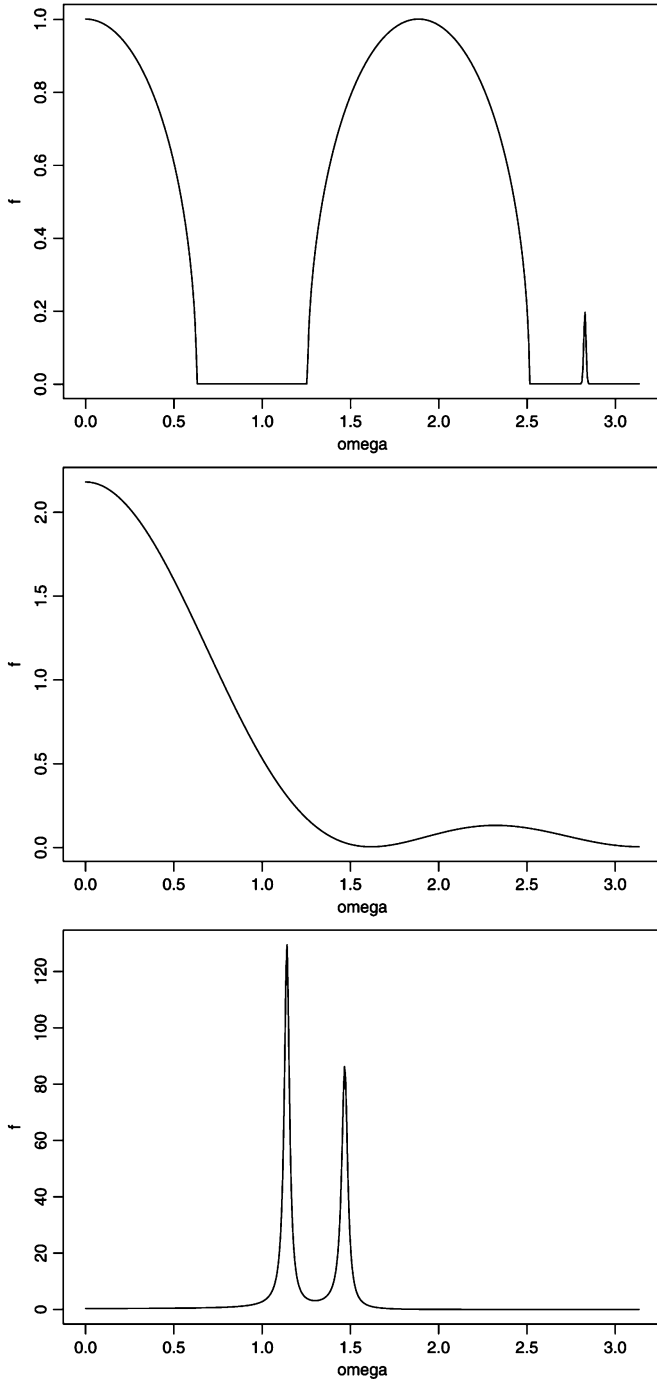


Fig. 1. Three testing spectra used in the numerical experiments. From top to bottom: The mobile radio communication example of [9], the broadband MA(3) example of [13], and the narrowband ARMA(4,4) example of [13].

Kullback–Leibler (KL) distance-based method of [7] while the second was the generalized cross-validation (GCV) method of [10]. Lastly, we also applied the recent cepstrum thresholding technique of [5] (see also [12]) to obtain a fourth estimate of f .

For each estimated spectrum, we calculated the corresponding mean-squared error (MSE), i.e., $(1/n) \sum (f_j - \hat{f}_{j,\alpha})^2$, for the sharpened estimate and similarly for the other three unsharpened estimates. The averaged MSEs together with their standard errors for each of the 12 combinations of experimental setups are tabulated in Table I. To summarize the relative performances of the above four estimators, we ranked them in the following manner. First, paired t -tests were applied to test if the

difference between the averaged MSE values of any two estimators is significant or not. The significance level used was 1.25%. If the averaged MSE value of a method is significantly less than the remaining three, it will be assigned a rank 1. If the averaged MSE value of a method is significantly larger than one but less than two methods, it will be assigned a rank 2, and similarly for ranks 3 and 4. Methods having nonsignificantly different averaged MSE values will share the same averaged rank. The resulting rankings are also tabulated in Table I.

The following empirical conclusions can be drawn. First, as the sample size increases, the performances of all estimators improve. Second, as the overall averaged pairwise t -test rankings for the proposed sharpened estimator, the KL estimator of [7], the GCV estimator of [10], and the cepstrum thresholding estimator of [5] are 1.08, 2.5, 2.42, and 4.0, respectively, there is some evidence suggesting that the proposed sharpened estimator is preferred. Third, for the mobile radio communication spectrum, the performances of the proposed estimator is much better than the rest, especially for large n . It is most likely due to the sharp spike feature of the spectrum, which, as a result of smoothing, can potentially cause large bias and the sharpening has successfully reduced it. Lastly, we want to comment on the poor performance of the cepstrum thresholding approach. As with most cepstrum approaches, this estimator aims to obtain a good estimate for the log of the spectrum; hence, it has a tendency to oversmooth sharp features in the spectrum.

VII. CONCLUDING REMARKS

In this correspondence, we have developed a new method for spectral density estimation via the smoothing of sharpened periodograms. We have shown theoretically that the smoothing of sharpened periodograms can reduce the bias to a higher order while at the same time only inflate the variance by a constant multiple. Using the idea of unbiased risk estimation, we have also constructed a method for choosing the two free tuning parameters involved in the estimation procedure, namely the bandwidth that determines the amount of smoothing and the sharpening parameter that controls the extent for sharpening. Numerical results suggest that sharpened estimates are superior to their unsharpened counterparts. One possible extension of the current work is to adopt other smoothing methods, such as wavelet shrinkage, to smooth the sharpened periodograms. This would require the development of new methods for bandwidth and sharpening parameter selection.

APPENDIX PROOFS

Proof of Lemma 1: We first show that A1) and A2) imply that, when $n \rightarrow \infty$

$$\begin{aligned} \sum_{m=-n}^{2n-1} W_{m-j}^2 &= \frac{\|K\|^2}{nh} + o\left(\frac{1}{nh}\right) \\ \sum_{m=-n}^{2n-1} W_{m-j}(\omega_m - \omega_j)^2 &= \sigma_K^2 h^2 + o(h^2). \end{aligned} \quad (11)$$

Let $s_l(\omega_j; h) = (\pi/n) \sum_{m=-n}^{2n-1} (\omega_m - \omega_j)^l K_h(\omega_m - \omega_j)$, where $K_h(\cdot) = (1/h)K(\cdot/h)$. Since $K^{(1)}$ is bounded on its compact support, say $[-M, M]$, for large n , $s_l(\omega_j; h)$ can be well approximated by

$$\begin{aligned} s_l(\omega_j; h) &= \int_{-\pi}^{2\pi} (y - \omega_j)^l K_h(y - \omega_j) dy + o(1/n) \\ &= h^l \int_{(-\pi - \omega_j)/h}^{(2\pi - \omega_j)/h} u^l K(u) du + o(1/n) \\ &= h^l \int_{-M}^M u^l K(u) du + o(1/n) = \mu_l(K) h^l + o(1/n) \end{aligned}$$

where $\mu_l(K) = \int u^l K(u) du$. Analogously, let $s_l^*(\omega_j; h) = (\pi/n) \sum_{m=-n}^{2n-1} (\omega_m - \omega_j)^l K_h^2(\omega_m - \omega_j)$, one has $s_l^*(\omega_j; h) =$

TABLE I

AVERAGE MSEs AND PAIRWISE t -TEST RANKINGS (IN ITALICS) OBTAINED FROM THE NUMERICAL EXPERIMENTS. NUMBERS IN PARENTHESES ARE STANDARD ERRORS, MULTIPLIED BY 10^4 , OF THE MSEs. THE FOUR ESTIMATORS WERE SHARP—THE PROPOSED SHARPENED ESTIMATOR, KL—THE UNSHARPENED ESTIMATOR WITH KL CHOICE OF BANDWIDTH [7], GCV—THE UNSHARPENED ESTIMATOR WITH GCV CHOICE OF BANDWIDTH [10], AND CEPS—THE CEPSTRUM THRESHOLDING APPROACH OF [5]. NOTICE THAT FOR BROADBAND MA(3) WITH $n = 18$, ALTHOUGH THE **ORAL** AVERAGED MSE OF SHARP IS LARGER THAN THOSE OF KL AND GCV, THE **PAIR** t -TEST HAS ASSIGNED IT A RANK OF 1

n	mobile radio communication				broadband MA(3)				narrowband ARMA(4,4)			
	Sharp	KL	GCV	Ceps	Sharp	KL	GCV	Ceps	Sharp	KL	GCV	Ceps
128	0.0376 (1.27) <i>1</i>	0.0451 (1.07) <i>2</i>	0.0806 (1.74) <i>3</i>	0.365 (14.2) <i>4</i>	0.0863 (7.97) <i>1</i>	0.0638 (2.76) <i>2</i>	0.0741 (3.13) <i>3</i>	0.229 (7.42) <i>4</i>	100 (4170) <i>1</i>	130 (1070) <i>3</i>	108 (1900) <i>2</i>	166 (703) <i>4</i>
256	0.0228 (0.830) <i>1</i>	0.0410 (0.799) <i>2</i>	0.0622 (1.14) <i>3</i>	0.217 (6.14) <i>4</i>	0.0454 (3.70) <i>1.5</i>	0.0459 (1.55) <i>3</i>	0.0437 (1.53) <i>1.5</i>	0.167 (4.59) <i>4</i>	78.9 (4070) <i>1.5</i>	95.5 (1080) <i>3</i>	86.0 (1460) <i>1.5</i>	166 (818) <i>4</i>
512	0.0132 (0.373) <i>1</i>	0.0384 (0.524) <i>2</i>	0.0479 (0.684) <i>3</i>	0.162 (3.60) <i>4</i>	0.0209 (1.42) <i>1</i>	0.0291 (1.04) <i>3</i>	0.0261 (0.961) <i>2</i>	0.0869 (2.54) <i>4</i>	50.1 (2020) <i>1</i>	56.7 (719) <i>2</i>	59.0 (755) <i>3</i>	143 (920) <i>4</i>
1024	0.00798 (0.185) <i>1</i>	0.0355 (0.332) <i>3</i>	0.0344 (0.381) <i>2</i>	0.105 (1.87) <i>4</i>	0.0116 (0.734) <i>1</i>	0.0171 (0.484) <i>3</i>	0.0149 (0.422) <i>2</i>	0.0460 (1.33) <i>4</i>	29.8 (1130) <i>1</i>	36.2 (547) <i>2</i>	40.6 (554) <i>3</i>	115 (783) <i>4</i>

$\mu(K^2)h^{l-1} + o(1/n)$. Note from A3 $\liminf nh^2 > 0$ which allows $o(1/n)$ to be replaced by $o(h^2)$, $\sum_{m=-n}^{2n-1} W_{m-j}^2 = s_0^*(\omega_j; h)/\{ns_0(\omega_j; h)\}$ and $\sum_{m=-n}^{2n-1} W_{m-j}(\omega_m - \omega_j)^2 = s_2(\omega_j; h)/s_0(\omega_j; h)$; hence, (11) is proved.

We now derive (8). A direct application of the Taylor expansion gives

$$f_m = f_j + (\omega_m - \omega_j)f_j^{(1)} + \frac{1}{2}(\omega_m - \omega_j)^2 f_j^{(2)} + o(n^{-2}).$$

For convenience, we shall write " $\sum_{m=-n}^{2n-1}$ " as " \sum_m " in the sequel unless defined otherwise. Thus

$$\begin{aligned}
 \text{Bias}(\hat{f}_j) &= \sum_m W_{m-j} \{E(f_m \epsilon_m) - f_j\} \\
 &= \sum_m W_{m-j} (f_m - f_j) \\
 &= \sum_m W_{m-j} \left\{ (\omega_m - \omega_j) f_j^{(1)} \right. \\
 &\quad \left. + \frac{1}{2}(\omega_m - \omega_j)^2 f_j^{(2)} + o\left(\frac{1}{n^2}\right) \right\} \\
 &= \frac{1}{2} \sigma_K^2 f_j^{(2)} h^2 + o(h^2) \\
 \text{Var}(\hat{f}_j) &= \text{Var}\left(\sum_m W_{m-j} I_m\right) = \sum_m W_{m-j}^2 f_m^2 \\
 &= \sum_m W_{m-j}^2 \left\{ f_j + (\omega_m - \omega_j) f_j^{(1)} + o\left(\frac{1}{n}\right) \right\}^2 \\
 &= \sum_m W_{m-j}^2 f_j^2 + o\left(\frac{1}{nh}\right) = \frac{\|K\|^2 f_j^2}{nh} + o\left(\frac{1}{nh}\right).
 \end{aligned}$$

Proof of Theorem 1: Under assumptions A1[†] and A2[†], by similar derivation of Lemma 1, and by applying the Taylor expansion up to the term h^4 , it is straightforward to show that

$$\hat{f}_m = f_m + \frac{1}{2} \sigma_K^2 f_m^{(2)} h^2 + \frac{1}{24} \mu_4(K) f_m^{(4)} h^4 + R_{n,m}$$

where $\mu_4(K) = \int u^4 K(u) du$, and $R_{n,m}$ is the remaining term satisfying $E(R_{n,m}) = o(h^4)$ and $\text{Var}(R_{n,m}) = O\{1/(nh)\}$. This implies that the sharpened periodograms can be expressed by

$$\begin{aligned}
 \tilde{I}_{m,\alpha} &= \{(1+\alpha)\epsilon_m - \alpha\} f_m - \frac{1}{2} \alpha \sigma_K^2 f_m^{(2)} h^2 \\
 &\quad - \frac{1}{24} \alpha \mu_4(K) f_m^{(4)} h^4 - \alpha R_{n,m}. \quad (12)
 \end{aligned}$$

One also has $f_m^{(2)} = f_j^{(2)} + (\omega_m - \omega_j) f_j^{(3)} + (\omega_m - \omega_j)^2 f_j^{(4)}/2 + o(n^{-2})$, and $f_m^{(4)} - f_j^{(4)} = o(1)$. Therefore

$$\begin{aligned}
 \text{Bias}(\tilde{f}_{j,\alpha}) &= \sum_m W_{m-j} \left[E\{(1+\alpha)\epsilon_m - \alpha\} f_m - \frac{1}{2} \alpha \sigma_K^2 f_m^{(2)} h^2 \right. \\
 &\quad \left. - \frac{1}{24} \alpha \mu_4(K) f_m^{(4)} h^4 - \alpha E(R_{n,m}) - f_j \right] \\
 &= \sum_m W_{m-j} \left\{ f_m - f_j - \frac{1}{2} \alpha \sigma_K^2 f_m^{(2)} h^2 \right. \\
 &\quad \left. - \frac{1}{24} \alpha \mu_4(K) f_m^{(4)} h^4 + o(h^4) \right\} \\
 &= \sum_m W_{m-j} \left[\left\{ \frac{1}{2} (\omega_m - \omega_j)^2 f_j^{(2)} + \frac{1}{24} (\omega_m - \omega_j)^4 f_j^{(4)} \right\} \right. \\
 &\quad \left. - \frac{1}{2} \alpha \sigma_K^2 h^2 \left\{ f_j^{(2)} + \frac{1}{2} (\omega_m - \omega_j)^2 f_j^{(4)} + o(n^{-2}) \right\} \right. \\
 &\quad \left. - \frac{1}{24} \alpha \mu_4(K) f_j^{(4)} h^4 + o(h^4) \right] \\
 &= \frac{1}{2} (1-\alpha) \sigma_K^2 f_j^{(2)} h^2 \\
 &\quad + \frac{1}{4} \left\{ \frac{1}{6} (1-\alpha) \mu_4(K) - \alpha \sigma_K^4 \right\} f_j^{(4)} h^4 + o(h^4).
 \end{aligned}$$

The asymptotic variance of $\tilde{f}_{j,\alpha}$ is given by

$$\begin{aligned}
 \text{Var}(\tilde{f}_j) &= \text{Var}\left[\sum_m W_{m-j} \left[\{(1+\alpha)\epsilon_m - \alpha\} f_m - \frac{1}{2} \alpha \sigma_K^2 f_m^{(2)} h^2 \right. \right. \\
 &\quad \left. \left. - \frac{1}{24} \alpha \mu_4(K) f_m^{(4)} h^4 - \alpha R_{n,m} \right] \right] \\
 &= \sum_m W_{m-j}^2 (1+\alpha)^2 f_m^2 + o\left(\frac{1}{nh}\right) \\
 &= \sum_m W_{m-j}^2 (1+\alpha)^2 \left\{ f_j + (\omega_m - \omega_j) f_j^{(1)} \right\}^2 + o\left(\frac{1}{nh}\right) \\
 &= (1+\alpha)^2 \frac{\|K\|^2 f_j^2}{nh} + o\left(\frac{1}{nh}\right).
 \end{aligned}$$

Proof of Theorem 2: First, we stress that the unbiasedness stated in this theorem only holds under model (1). The proof begins by noting that $E\{\text{RSS}(h, \alpha)\} = E\{\sum_j (I_j - \tilde{f}_{j,\alpha})^2\} = \sum_j E(I_j^2 - 2I_j\tilde{f}_{j,\alpha} + \tilde{f}_{j,\alpha}^2)$. Since the ϵ_j 's are independent standard exponentials, then $E(I_j) = f_j$, $E(I_j^2) = E(f_j^2 \epsilon_j^2) = 2f_j^2$. From (3) and (5), one has $\tilde{I}_{j,\alpha} = (1 + \alpha)I_j - \alpha \sum_m W_{m-j} I_m$ and

$$\tilde{f}_{j,\alpha} = (1 + \alpha) \sum_{m=-n}^{2n-1} W_{m-j} I_m - \alpha \sum_{m,k=-n}^{2n-1} W_{m-j} W_{k-m} I_k.$$

Then

$$\begin{aligned} E(I_j \tilde{f}_{j,\alpha}) &= E \left\{ (1 + \alpha) f_j \epsilon_j \sum_m W_{m-j} f_m \epsilon_m \right\} \\ &\quad - \alpha E \left(f_j \epsilon_j \sum_{m,k} W_{m-j} W_{k-m} f_k \epsilon_k \right) \\ &= (1 + \alpha) \left(f_j \sum_{m \neq j} W_{m-j} f_m + 2W_0 f_j^2 \right) \\ &\quad - \alpha \left(2 \sum_m W_{m-j} f_j^2 + f_j \sum_{k \neq j} W_{m-j} W_{k-m} f_k \right) \\ &= \left\{ (1 + \alpha) W_0 - \alpha \sum_m W_{m-j}^2 \right\} f_j^2 + f_j \\ &\quad \times \left\{ (1 + \alpha) \sum_m W_{m-j} f_m - \alpha \sum_{m,k} W_{m-j} W_{k-m} f_k \right\} \\ &= \left\{ (1 + \alpha) W_0 - \alpha \sum_m W_{m-j}^2 \right\} f_j^2 + f_j E(\tilde{f}_{j,\alpha}). \end{aligned}$$

Therefore

$$\begin{aligned} E\{(I_j - \tilde{f}_{j,\alpha})^2\} &= 2f_j^2 - 2 \left[\left\{ (1 + \alpha) W_0 - \alpha \sum_m W_{m-j}^2 \right\} f_j^2 \right. \\ &\quad \left. + f_j E(\tilde{f}_{j,\alpha}) \right] + E(\tilde{f}_{j,\alpha}^2) \\ &= E\{(f_j - \tilde{f}_{j,\alpha})^2\} \\ &\quad - \left[2 \left\{ (1 + \alpha) W_0 - \alpha \sum_m W_{m-j}^2 \right\} - 1 \right] f_j^2, \end{aligned}$$

and

$$\begin{aligned} E\{\text{RSS}(h, \alpha)\} &= nR(h, \alpha) - \sum_{j=0}^{n-1} \left[2 \left\{ (1 + \alpha) W_0 - \alpha \sum_m W_{m-j}^2 \right\} - 1 \right] f_j^2. \end{aligned}$$

Thus, $\hat{R}(h, \alpha)$ defined in (7) is an unbiased estimator of $R(h, \alpha)$.

ACKNOWLEDGMENT

The authors dedicate this correspondence to P. Brockwell for his retirement. Comments from the referees are gratefully acknowledged.

REFERENCES

- [1] P. J. Brockwell and R. A. Davis, *Time Series: Theory and Methods*, 2nd ed. New York: Springer-Verlag, 1991.
- [2] E. Choi and P. Hall, "Data sharpening as a prelude to density estimation," *Biometrika*, vol. 86, pp. 941–947, 1999.
- [3] E. Choi, P. Hall, and V. Rousson, "Data sharpening methods for bias reduction in nonparametric regression," *Ann. Stat.*, vol. 28, pp. 1339–1355, 2000.
- [4] T. Gasser, H.-G. Müller, and V. Marmittsch, "Kernels for nonparametric curve estimation," *J. Roy. Stat. Soc. Series B*, vol. 47, pp. 238–252, 1985.
- [5] E. Gudmundson, N. Sandgren, and P. Stoica, "Automatic smoothing of periodograms," in *Proc. 31st Int. Conf. Acoustics, Speech, Signal Processing*, 2006, pp. 504–507.
- [6] P. Hall and M. C. Minnotte, "High order data sharpening for density estimation," *J. Roy. Stat. Soc. Series B*, vol. 64, pp. 141–157, 2002.
- [7] J. Hannig and T. C. M. Lee, "Kernel smoothing of periodograms under Kullback–Leibler discrepancy," *Signal Process.*, vol. 84, pp. 1255–1266, 2004.
- [8] T. C. M. Lee, "A simple span selector for periodogram smoothing," *Biometrika*, vol. 84, pp. 965–969, 1997.
- [9] P. Moulin, "Wavelet thresholding techniques for power spectrum estimation," *IEEE Trans. Signal Process.*, vol. 42, no. 11, pp. 3126–3136, Nov. 1994.
- [10] H. C. Ombao, J. A. Raz, R. L. Strawderman, and R. von Sachs, "A simple generalised crossvalidation method of span selection for periodogram smoothing," *Biometrika*, vol. 88, pp. 1186–1192, 2001.
- [11] K. S. Riedel and A. Sidorenko, "Adaptive smoothing of the log-spectrum with multiple tapering," *IEEE Trans. Signal Process.*, vol. 44, no. 7, pp. 1794–1800, Jul. 1996.
- [12] P. Stoica and N. Sandgren, "Smoothed nonparametric spectral estimation via cepstrum thresholding," *IEEE Signal Process. Mag.*, 2006, to be published.
- [13] P. Stoica and T. Sundin, "Optimally smoothed periodogram," *Signal Process.*, vol. 78, pp. 253–264, 1999.
- [14] G. Wahba, "Automatic smoothing of the log periodogram," *J. Amer. Stat. Assoc.*, vol. 75, pp. 122–132, 1980.